Rapid carrier relaxation in self-assembled $In_xGa_{1-x}As/GaAs$ quantum dots

B. Ohnesorge, M. Albrecht, J. Oshinowo, and A. Forchel
Technische Physik, Universität Würzburg, Am Hubland, 97074 Würzburg, Germany

Y. Arakawa
Institute of Industrial Science, University of Tokyo, 7-22-1 Roppongi, Minato-ku, Tokyo 106, Japan
(Received 19 January 1996; revised manuscript received 21 June 1996)

Carrier capture and relaxation processes in self-assembled 15-nm $In_{0.5}Ga_{0.5}As/GaAs$ quantum dots are investigated by means of time-resolved photoluminescence spectroscopy. In a systematic study of photoluminescence rise times and barrier decay times (variation of temperature, excitation energy, and excitation density) we aim to identify the physical mechanisms responsible for fast carrier capture and relaxation in quantum dots. Both processes are separated by using appropriate excitation energies. Carrier capture and relaxation are shown to proceed with rates as high as $\sim 2\times 10^{10}$ s^{-1} at low temperature even if less than one electron-hole pair per dot and excitation pulse is created. We interpret our results in terms of multiphonon processes at low excitation densities and in terms of Auger processes at high excitation densities. [S0163-1829(96)03240-7]

I. INTRODUCTION

Among the fundamental properties of zero-dimensional semiconductor structures carrier relaxation processes have been widely discussed because of their physical interest and their important implications on the luminescence efficiency and performance of potential applications such as quantum dot lasers. Due to the discrete nature of the electron and hole energy levels of quantum dots (QD's), single longitudinal-optical (LO) -phonon emission is forbidden, except in the unlikely case that energy levels are separated by the phonon energy $\hbar\omega_{\mathrm{LO}}$. Single longitudinal-acoustic (LA) -phonon emission by deformation potential coupling is strongly quenched with decreasing dot size as soon as the energy-level separation exceeds a few meV.[1] Recently, coupling between electrons and LA phonons arising from the perturbation of the electron wave function by the motion of QD interfaces has been studied and shown to dominate the deformation potential coupling for dot sizes less than ~ 50 nm.[2] But still, the overall magnitude of the scattering time for both mechanisms is much larger than typical QD recombination times of about 1 ns because the momentum of the single acoustic phonon required to cover large QD energy separations in small dots cannot be supplied by the electron with its relatively large wavelength of the order of the dot size. Poor luminescence properties[3] and luminescence from excited QD states[4,5] have been attributed to this ''phonon bottleneck effect.''

Recently the growth and characterization of self-assembled QD's (Stranski-Krastanow growth mode) has attracted much interest.[6–9] Due to the strong carrier confinement leading to a small number of states well separated by at least a few tens of meV for electrons *and* holes these quantum dots constitute ideal objects to study relaxation mechanisms in the full ''bottleneck regime.'' In addition, the high quantum efficiency of such self-assembled QD's allows one to use very low excitation densities such that the relaxation of single electron-hole pairs per dot and excitation pulse can be investigated. Early time-resolved studies using nonresonant excitation energies report a fast photoluminescence (PL) rise time, suggesting that the phonon bottleneck is overcome by the presence of an alternative, efficient carrier relaxation process in these self-assembled QD's.[10,11] Auger processes were proposed to provide an efficient relaxation,[11,12] but have not yet been identified experimentally by their characteristic temperature and density dependence. In addition, it has been shown theoretically[13] that electrons can efficiently interact with LO phonons in a wide energy range (>50 meV) when applying coupled equations in Wigner-Weisskopf theory instead of Fermi's golden rule as generally used in discussions of the phonon bottleneck.[1,2]

In this paper we present a systematic study of the PL rise times of self-assembled $In_xGa_{1-x}As/GaAs$ quantum dots after pulsed picosecond excitation as a function of temperature excitation density, and excitation energy. By variation of the excitation energy we are able to separate carrier capture, carrier relaxation, and carrier recombination processes. As a result, capture and relaxation processes are shown to be fast, i.e., of the order of 2×10^{10} s^{-1}, even in the regime of less than a single electron-hole pair per dot under resonant excitation, where Auger processes can be excluded. We are able to explain our temperature-dependent rise-time measurements for different excitation densities at low excitation densities by a multiphonon relaxation process that involves characteristic LA phonons of 2.7 meV and by Auger processes at high excitation densities.

The paper is organized as follows. After a description of the samples and the experimental setup in Sec. II and a brief cw optical characterization of the QD's in Sec. III, the results of the time-resolved measurements are discussed in two main parts. In Sec. IV we compare PL rise times under resonant and nonresonant excitation with the decay times of the GaAs barrier for different temperatures allowing us to identify the time scales for carrier capture and carrier relaxation. Section V aims at identifying the physical mechanisms that are responsible for the fast carrier capture and relaxation by using the experiments at different temperatures and excitation densities.

II. SAMPLES AND EXPERIMENTAL SETUP

The samples were grown by the metal-organic chemical vapor deposition growth technique on a GaAs substrate.[6] On top of a 200-nm GaAs buffer layer two-dimensional $In_{0.5}Ga_{0.5}As$ was deposited. Due to the large lattice mismatch, the surface transforms into three-dimensional islands (Stranski-Krastanow growth mode) after the deposition of 1.5 monolayers (ML). Scanning electron and atomic force micrography reveal the formation of dots with a narrow size distribution. The dot diameter is about 15 nm, the dot height about 5 nm before overgrowth, and the area dot density about 2×10^9 cm^{-2}. The dots were covered in one growth run by a 30-nm GaAs cap barrier layer using a lower growth temperature. A reference $In_{0.17}Ga_{0.83}As/GaAs$ quantum well (QW) of 5 nm thickness was grown under similar growth conditions. Details of the sample growth are reported in Ref. 6. From part of the QD sample the GaAs cap, the QD layer, and $\sim$30 nm of the GaAs buffer were removed by wet chemical etching.

Time-resolved optical experiments were performed in the temperature range between 2 and 80 K. Nonresonant and resonant excitation were provided by the second harmonic of a continuously mode-locked and pulse-compressed Nd:YAG laser (where YAG denotes yttrium aluminum garnet) (3 ps pulses at 532 nm) and by a wavelength-tunable, continuously mode-locked Ti:sapphire laser (1.5-ps pulses in the 720–1080 nm range), both with a repetition rate of 82 MHz. The PL signal was dispersed by a $f=25$ cm monochromator with a spectral resolution of about 0.5 meV and detected with a synchroscan streak camera. The temporal resolution of the setup amounts to about 10 ps. The photoluminescence excitation (PLE) spectrum was recorded using a cw Ti:sapphire laser, a $f=1$ m double monochromator, and a Ge detector.

III. cw OPTICAL CHARACTERIZATION

The cw photoluminescence (thick lines) and photoluminescence excitation spectra (thin lines) of the unprocessed dot sample are given in Fig. 1. The luminescence at 1.34 eV of a large number of dots excited in the focus of the laser of $\sim$100 μm diameter has a narrow linewidth of 25 meV reflecting the high quality of the dots. Micro-PL measurements systematically reducing the number of dots under optical investigation (etched mesas) show sharp photoluminescence lines from individual quantum dots as observed by other groups[7–9] and clearly demonstrate that the inhomogeneously broadened macro-PL arises from a superposition of these sharp PL lines from zero-dimensional states with slightly different energies. The dot emission shifts to lower energies with increasing temperature similarly to the energy shift of the reference QW,[6] giving no indication of defect formation in our dot sample. We emphasize that under nonresonant excitation conditions the integrated emission intensity of the dots is nearly as high as the total emission intensity of the reference QW. Furthermore, no PL signal of the $In_xGa_{1-x}As$ wetting layer is resolved below the GaAs barrier. This demonstrates an efficient carrier capture and a very high quantum yield of the dots.

The PLE spectrum (thin lines in Fig. 1) is detected at $E_{det}=1.333$ eV near the center of QD photoluminescence and expanded near the GaAs barrier in the inset. The absorption peak below the GaAs barrier exciton is interpreted as due to the $In_xGa_{1-x}As$ wetting layer (WL). Its energetic position at 1.512 eV and the position of the QD emission at 1.34 eV indicate that the actual indium content in our structure is around 30%. Reducing the excitation energy below the wetting-layer ground state, the PLE signal drops significantly by about an order of magnitude since absorption can now only take place in the $In_xGa_{1-x}As$ quantum dots.

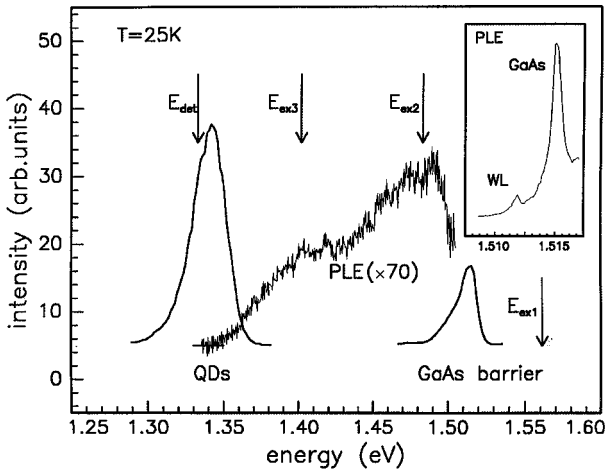

FIG. 1. Low-temperature (25 K) time-integrated PL spectrum (thick lines) of the $In_{0.5}Ga_{0.5}As/GaAs$ dot sample under nonresonant excitation ($E_{ex}=2.330$ eV and $I=2.5$ W/cm^2) and corresponding photoluminescence excitation (PLE) spectrum of the QD luminescence (thin lines). The inset is an expanded view of the PLE spectrum near the GaAs barrier showing the wetting layer (WL) absorption. Arrows indicate the three excitation energies relevant for Fig. 3 and the detection energy for the PLE spectrum.

The resonant part of the PLE spectrum exhibits two rather broad structures that we attribute to excited QD states. Transitions between the electronic states and the various light-hole and heavy-hole states should conserve the azimuthal but not necessarily the radial quantum number in the dots with cylindrical symmetry. We therefore expect that many allowed excited-state transitions contribute to the excitation spectrum.[14] The large number of probed QD's that may have the same ground-state energy but different excited-state energies due to independent fluctuations of size, shape, In content, and strain gives rise to the inhomogeneously broadened structures in the excitation spectrum. We do not observe any PL enhancement for excitation energies permitting single LO-phonon relaxation as Fafard *et al.*[15] and Raymond *et al.*[16] reported for some of their presented samples, indicating that the interlevel spacing and phonon energies are not closely matched in our dot sample.

Model calculations of the excitonic eigenstates and energies in the spherically shaped dots[14] indicate that the first excited state is about 40 meV above the excitonic ground state. We therefore exclude any emission from excited states to be present in our photoluminescence signal. Finally, it is important to note that there is virtually no observable signal when exciting within the PL emission line. This is a clear sign of the sharp zero-dimensional density of states of the QD's, which prevents observing time-integrated PL from QD's directly excited in their ground states due to scattered laser light.

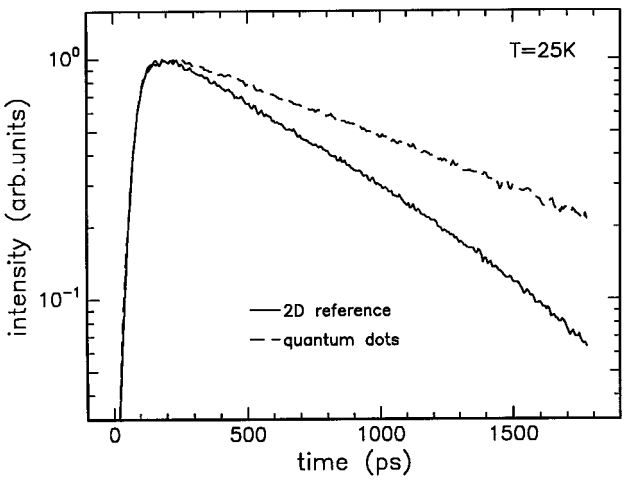

FIG. 2. Time-resolved PL emission of the QD's and the reference QW at low temperature ($T=25$ K) under resonant excitation $E_{ex2}=1.483$ eV ($I=75$ W/cm^2).

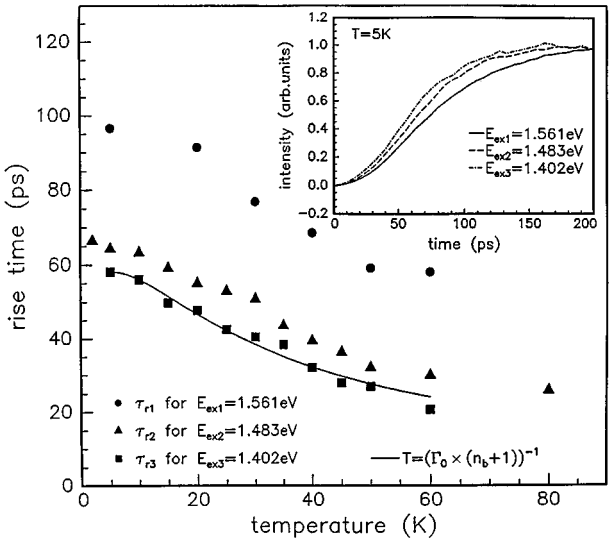

FIG. 3. Temperature dependence of the QD rise times for the three excitation energies of Fig. 1 under low excitation density of less than one electron-hole pair per dot and excitation pulse ($I_1=2.5$ W/cm^2 and $I_2=I_3=75$ W/cm^2). The solid fit curve using a Bose distribution function is described in Sec. V A. The inset shows the temporal rise of the QD photoluminescence signal for the three excitation energies at $T=5$ K.

IV. IDENTIFICATION OF CARRIER CAPTURE AND CARRIER RELAXATION

Figure 2 depicts the time-resolved variation of the emission intensity of the QD's and the reference QW ($T=25$ K, resonant excitation energy $E_{ex}=1.483$ eV, and excitation intensity 75 W cm^{-2}) averaged over 7 meV (3.5 meV) at the center of the PL line of the QD's (QW). The traces exhibit fast rise times for the two-dimensional (2D) reference and the QD's. We observe a prolonged QD decay time ($\tau=1032$ ps) as compared to the QW decay time ($\tau=618$ ps). Throughout this paper we will apply a three-level model to analyze the temporal profiles. The carrier capture and relaxation from the excited state to the excitonic ground state and the excitonic lifetime are modeled by time constants τ_r and τ, respectively. The time evolution of the PL signal then follows from the analysis of the rate equations

$$I(t)\propto(e^{-t/\tau}-e^{-t/\tau_r})/(\tau-\tau_r). \tag{1}$$

Note that (1) is invariant against an interchange of τ_r and τ. The prolonged QD decay time can therefore either reflect a prolonged carrier lifetime or a slowed down carrier relaxation as predicted by the phonon bottleneck. The following studies will, however, confirm the first interpretation and show that the short QD rise time is determined by carrier capture and relaxation processes that are as fast as in the 2D reference QW.

The temporal rise of the QD photoluminescence signal is shown in the inset of Fig. 3 for three different excitation energies ($T=5$ K). As indicated by the arrows in Fig. 1, excitation energies above and below the GaAs band gap have been used. The PL rise times are determined from a curve fit of the whole temporal evolution of the PL emission according to Eq. (1). The slowest rise time of 93 ps corresponds to an excitation energy of 1.561 eV, slightly above the GaAs barrier band gap, while rise times of 62 and 56 ps are observed under resonant excitation at 1.483 eV below the ground state of the 1.5-ML $In_xGa_{1-x}As$ wetting layer and 1.402 eV deep in the dots, respectively. The resonant excitation energies (1.483 and 1.402 eV) correspond to the maxima of the cw photoluminescence excitation spectrum as discussed in Sec. III. The resonant excitation intensities were limited in order to restrict the average number of carriers created per dot to less than one electron-hole pair per dot and pulse (75 W cm^{-2}). Using a filling factor of 3.5×10^{-3} and an absorption coefficient of 5×10^6 m^{-1}, we estimate an average number of 0.2 pairs per dot and pulse for $I=75$ W cm^{-2}. Nonresonant excitation was then adjusted to yield approximately the same total intensity, i.e., the same number of electron-hole pairs per dot and pulse (~2.5 W cm^{-2}). Under these excitation conditions we observe the dynamics of single electron-hole pairs per dot and exclude many particle effects, as will be confirmed in Sec. V.

Figure 3 summarizes the rise times for the three different excitation energies as a function of temperature. Increasing temperature reduces all PL rise times systematically by approximately 35 ps between 5 and 60 K while preserving a constant offset of roughly 30 ps between rise times under nonresonant excitation just above the GaAs barrier and resonant excitation just below the $In_xGa_{1-x}As$ wetting layer. Exciting at still lower energies ($E_{ex}=1.402$ eV) decreases the rise times only slightly by some more 5–10 ps.

We now turn to a study of the barrier luminescence. For nonresonant excitation the electronic states in the QD's will be populated mainly by carriers excited in the GaAs barrier. This results in an important carrier loss mechanism for the barrier. Figure 4 shows time-resolved photoluminescence profiles of the GaAs barrier of the QD sample (solid line) and of the etched sample without the QD layer (dashed line) at $T=25$ K. An excitation energy of 2.330 eV was used in both cases. Due to the high absorption coefficient the laser penetration depth amounts to about 150 nm. Thus the GaAs emission originates mainly from the GaAs buffer layer. The lifetime of the GaAs barrier in the sample where the QD layer has been completely removed (dashed curve in Fig. 4)

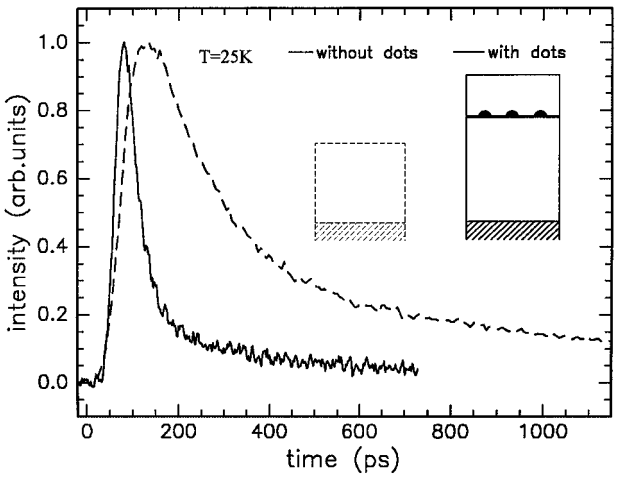

FIG. 4. Time-resolved photoluminescence signals of the GaAs barrier ($T=25$ K, $E_{ex}=2.33$ eV, and $I=2.5$ W/cm^2) before (solid curve, $\tau_{bar}=27$ ps) and after removal of the QD's (dashed curve, $\tau_0=216$ ps) as illustrated in the inset.

amounts to $\tau_0=216$ ps and is dominated by surface recombination and diffusion into the substrate where more nonradiative recombination channels might be present. In contrast, the lifetime of the GaAs emission in the original dot sample is drastically reduced to $\tau_{bar}=27$ ps (solid curve in Fig. 4). Note that an increase of the surface recombination velocity by the wet chemical etching process would result in the opposite effect, i.e., a shorter barrier lifetime for the sample without the QD's. Clearly, it is the presence of the QD layer that results in a fast loss channel for carriers in the GaAs barrier.

The efficient carrier capture is confirmed first by the high luminescence intensities of the QD's and second by a decrease of the time- and wavelength-integrated GaAs barrier signal with QD's by a factor of 3 as compared to the one without QD's. The absence of any emission from the 1.5-ML wetting layer in our sample indicates that carriers are not just captured into the wetting layer but are furthermore efficiently and rapidly transferred into the QD's. From the barrier lifetime of the unprocessed dot sample τ_{bar} we deduce a *capture time* τ_c for the carrier capture from the barrier into the QD's by taking into account the finite lifetime of the carriers in the barrier without QD's τ_0 according to $1/\tau_c=1/\tau_{bar}-1/\tau_0$. For the data shown in Fig. 4 we obtain a capture time of about 31 ps for $T=25$ K. Within these 31 ps carriers diffuse to the QD's and are captured into the high-lying QD states.

Figure 5 compares the carrier capture time τ_c obtained from the lifetime of the barrier (diamonds in Fig. 5) with the difference in rise times of the QD emission (circled triangles in Fig. 5) obtained by subtracting the rise times τ_{r2} under excitation slightly below the WL at $E_{ex}=1.483$ eV from the rise times τ_{r1} under excitation slightly above the GaAs band gap at $E_{ex}=1.561$ eV for different temperatures. The good agreement identifies the difference in rise times as the carrier capture time from the barrier into the QD's:

$$\tau_c=\tau_{r1}-\tau_{r2}. \tag{2}$$

It furthermore allows the following assignments, thereby resolving the ambiguities discussed with Eq. (1) and Fig. 2.

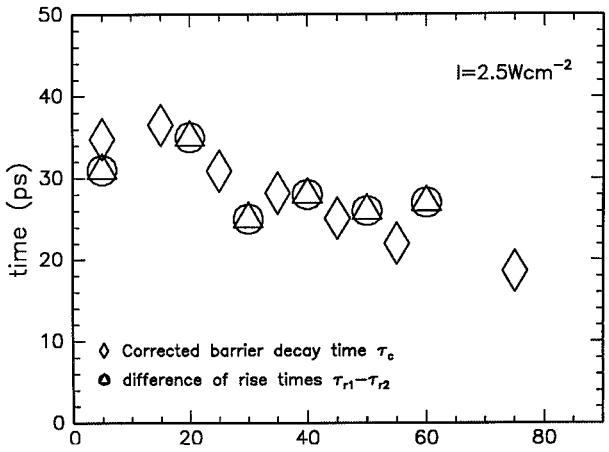

FIG. 5. Comparison of the corrected barrier decay time τ_c for $I=2.5$ W/cm^2 (see the text) with the difference in rise times $\tau_{r1}-\tau_{r2}$ from Fig. 3 as a function of temperature.

(i) PL rise times under nonresonant excitation are determined by carrier capture into the dots and carrier relaxation inside the dots while rise times under resonant excitation reflect the carrier relaxation inside the QD's solely. Equation (2) implies that the carrier relaxation process is the same for nonresonant and resonant excitation for the low excitation densities used (cf. Sec. V A).

(ii) PL decay times are determined by the exciton lifetime in the QD ground state. They remain constant at low temperature and are nearly independent of the excitation energy.

Consequently, we interpret the comparison of the time-resolved emission curves of the QD's and the QW of Fig. 2 as follows. (i) The nearly identical rise times of the two PL signals for 25 K (Ref. 17) is evidence that the carrier relaxation in the QD's is as fast as in the 2D reference QW. (ii) The prolonged QD decay time as compared to the one of the QW is an indication of the smaller coherence volume of the exciton in the QD.[18]

V. NATURE OF THE CARRIER CAPTURE AND RELAXATION MECHANISMS

Having identified the origin of the PL rise and decay times we want to further characterize the capture and relaxation processes present in our QD's in order to understand the underlying physical mechanisms. We therefore studied the PL rise times under nonresonant excitation [$E_{ex}=2.330$ eV (Ref. 19)] as a function of the excitation density as shown in Fig. 6. For excitation densities below ~ 4 W/cm^2 the PL rise times amount to about 90 ps and do not depend on excitation density. In contrast, for excitation densities above ~ 4 W/cm^2 nonresonant rise times are no longer independent of the excitation power: They decrease with increasing density dropping below 40 ps at 90 W/cm^2.

Figure 7 displays the temperature dependence of the PL rise times for the two typical excitation densities 2.5 and 50 W/cm^2 marked by arrows in Fig. 6 together with the temperature dependence of the corrected barrier decay time τ_c for the high excitation density. Under low excitation density (2.5 W/cm^2) the PL rise times decrease with increasing temperature (cf. Sec. IV), while temperature no longer affects

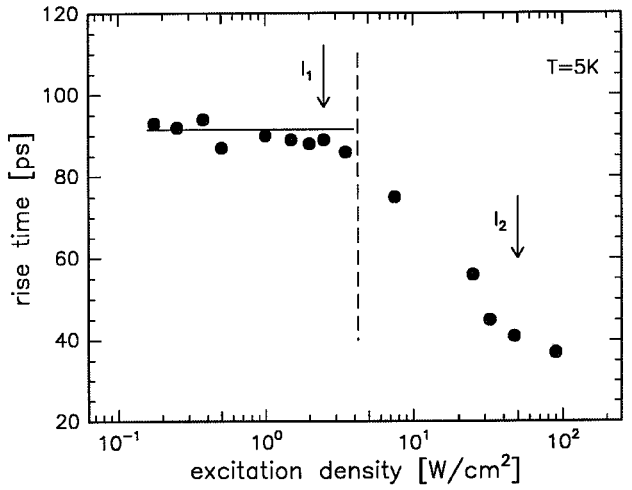

FIG. 6. Rise times of the QD photoluminescence under nonresonant excitation ($E_{ex}=2.330$ and $T=5$ K) as a function of the laser excitation density.

the carrier capture and relaxation processes under high excitation density (50 W/cm^2). In the latter case, rise times remain constant at about 40 ps and coincide with the corrected barrier decay time τ_c.

As demonstrated by Figs. 6 and 7, we deal with two density regimes with markedly different properties. (i) The PL rise times are independent of excitation density below ~ 4 W/cm^2 and depend on excitation density above ~ 4 W/cm^2. (ii) The PL rise times depend on temperature for $I=2.5$ W/cm^2 and are independent of temperature for $I=50$ W/cm^2. (iii) As shown in Sec. IV under low excitation density (2.5 W/cm^2) capture and carrier relaxation are separable, i.e., the sum of the rise time under resonant excitation τ_{r2} and the corrected barrier decay time τ_c equals the rise time under nonresonant excitation τ_{r1}:

$$\tau_{r2}+\tau_c=\tau_{r1}. \qquad (2')$$

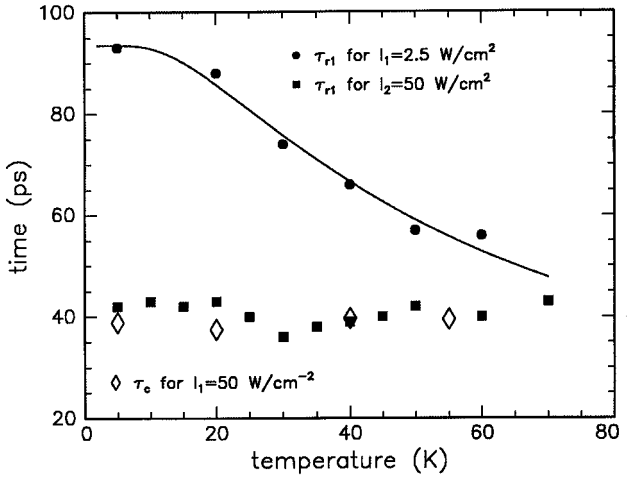

FIG. 7. Temperature dependence of the QD rise times τ_{r1} under nonresonant excitation for the two different excitation densities 2.5 and 50 W/cm^2 marked by arrows in Fig. 6. Also, the corrected barrier decay time τ_c for 50 W/cm^2 is shown.

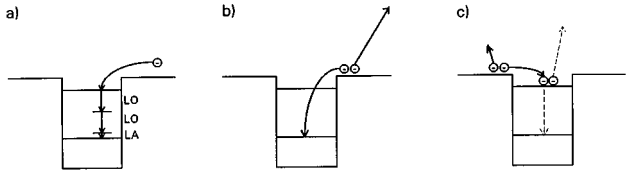

FIG. 8. Interpretation of the carrier capture and relaxation processes: (a) multiphonon processes under low excitation density, (b) single, and (c) sequential Auger processes under high excitation density.

Under high excitation density (50 W/cm^2) the nonresonant rise time and the corrected barrier decay time are identical, as shown in Fig. 7, as a function of temperature:

$$\tau_c=\tau_{r1}. \qquad (3)$$

The observed differences raise the question whether different mechanisms are responsible for the carrier relaxation in the two density regimes. In fact, we will show in the following that the carrier relaxation process is mediated by multiphonon processes under low excitation and by Auger processes under high excitation.

Beforehand, we want to investigate the average number of electron-hole pairs created in the QD's per excitation pulse again: The dynamics of the QD luminescence should considerably change as soon as state filling takes place.[20] First, the time evolution of the ground-state emission should show a plateaulike behavior due to carrier replenishment from higher states before following an exponential decay. Second, the transient spectra at short times after the pulsed excitation are expected to exhibit broadening on the high-energy side due to luminescence from excited states. Under nonresonant excitation at $E_{ex}=2.33$ eV both effects can first be seen very weakly at excitation densities $I \geqslant 7.5$ W/cm^2 in our sample. Hence the ''one electron-hole pair per dot and pulse'' regime is expected not much below the excitation density of 7.5 W cm^{-2}. Taking into account that the PL rise times do not change for excitation densities below 4 W cm^{-2} ranging down to densities as low as 0.2 W cm^{-2}, the relaxation dynamics in this regime is considered to essentially reflect the relaxation of single electron-hole pairs per dot. This will be particularly true for the lower nonresonant excitation energy $E_{ex1}=1.561$ eV used for the measurements of Fig. 3 ($I=2.5$ W cm^{-2}), yielding a six times larger absorption depth but the same PL rise times with the same temperature dependence. Therefore, the number of pairs per dot and excitation pulse of 0.2 calculated in Sec. IV seems realistic.

A. Multiphonon processes (low excitation density)

According to Eq. (2), carrier capture and relaxation are sequential processes under low excitation density (one electron-hole pair per dot and pulse). Carriers are first captured into the high-lying energy levels just below the wetting-layer continuum (probably by the emission of LO phonons) and relax inside the QD's afterward [Fig. 8(a)]. The latter process is the slower one and reveals a stronger temperature dependence: The carrier relaxation is accelerated by about 40 ps by increasing the temperature from 2 to 60 K (Fig. 3), while the carrier capture time decreases only by about 10 ps from ~ 35 to ~ 25 ps in the same temperature

range (Fig. 5). The main contribution to the temperature dependence of *all* PL rise times therefore stems from the temperature dynamics of the relaxation process inside the dots, which is obviously the same for nonresonant and resonant excitation.

Trying to identify the relaxation process, we first note that Auger processes with carriers in the surrounding barrier material should not be present under resonant excitation. Auger processes inside the QD are ruled out in the one electron-hole pair per dot regime because a third carrier is required to relax both the electron and hole energy. In fact, the temperature dependence of the PL rise times seems to be determined by a Bose distribution function $n_B=[\exp(E/kT)-1]^{-1}$, which is an indication for a phonon relaxation process. By using a function of the form $\tau^{-1}=\Gamma_0\times(n_B+1)$, where Γ_0 is the transition rate for $T=0$ K, we are able to perfectly reproduce the temperature-dependent rise times as shown in Fig. 3 for the lower resonant excitation energy. The fit yields a characteristic energy of $E=2.7$ meV. We point out that this energy compares favorably with the threshold LA-phonon energy for reduced relaxation in a QD,

$$\hbar\omega_k^{\max}\approx\hbar c_s(2\pi/L_z), \tag{4}$$

which has been deduced from energy and quasimomentum conservation arguments.[21] This energy has been shown to be effective in predicting the maximum LA emission rate in the direction of the strongest confinement L_z and the onset of strongly quenched LA transition rates at higher phonon energies for a statistical average of an ensemble of QD's. Using $L_z=5$ nm as the smallest dot dimension and a velocity of sound of $c_s=3400$ m/s for $In_{0.53}Ga_{0.47}As$,[21] we obtain $\hbar\omega_k^{\max}=2.8$ meV. We seem to deal with a relaxation process including the emission of acoustic phonons with an energy that is typical for the particular QD size and allows maximum emission rates. This is the case when the acoustic-phonon wavelength is comparable with the electron's wavelength according to Eq. (4). Because no intermediate electronic or excitonic states are available for both single such LA emission processes and single LO emission processes we assign the fast relaxation to multiphonon processes of several LO and LA phonons [Fig. 8(a)] as recently observed in PLE experiments.[22]

In an attempt to further test the idea of a multiphonon relaxation process we investigate the probability of an electron to emit one LO phonon $\hbar\omega_q^{\mathrm{LO}}$ and one LA phonon $\hbar\omega_k^{\mathrm{LA}}$ in a two-phonon process:[23]

$$W_{\mathrm{em}}=\frac{1}{\tau}=\frac{2\pi}{\hbar}\sum_{q,k}\left|\sum_s{}'\left(\frac{M_q^{is}M_k^{sf}}{E_i-E_s-\hbar\omega_q^{\mathrm{LO}}}+\frac{M_k^{is}M_q^{sf}}{E_i-E_s-\hbar\omega_k^{\mathrm{LA}}}\right)\right|^2[n_B(\hbar\omega_q^{\mathrm{LO}})+1][n_B(\hbar\omega_k^{\mathrm{LA}})+1]\delta(E_i-E_f-\hbar\omega_q^{\mathrm{LO}}-\hbar\omega_k^{\mathrm{LA}}), \tag{5}$$

where n_B, $\hbar\omega_q^{\mathrm{LO}}$ ($\hbar\omega_k^{\mathrm{LA}}$), and M_q (M_k) are the Bose distribution function, the LO (LA) phonon energy, and the matrix elements for LO (LA) emission via the Fröhlich interaction (deformation potential interaction), respectively. i (f) denotes the initial (final) QD state and s a virtual intermediate state. The following arguments can then be generalized to higher-order multiphonon processes.

(i) The temperature dependence of a two-phonon emission rate is determined by the products $[n_B(\hbar\omega_q^{\mathrm{LO}})+1][n_B(\hbar\omega_k^{\mathrm{LA}})+1]$. In the investigated temperature regime below 80 K we have $\hbar\omega_q^{\mathrm{LO}}\gg kT\approx\hbar\omega_k^{\mathrm{LA}}$ and the LO Bose functions are negligible. Acoustic phonons $\hbar\omega_k^{\max}$ with the maximum relaxation rate will give the major contribution to the sum over acoustic wave vectors k and dominate the temperature dependence of the whole emission rate as observed experimentally:

$$W_{\mathrm{em}}\propto[n_B(\hbar\omega_k^{\max})+1]. \tag{6}$$

However, we cannot exclude the participation of more than one LA phonon in a multiphonon process because the measured rise times can be fitted by products of the form (6) with slightly higher phonon energies as well.

(ii) We recall that single LA emission rates should not exceed 10^7 s^{-1} due to the small matrix elements M_k^{LA}, while single LO processes proceed on a subpicosecond time scale at $T=0$ K (large matrix elements M_q^{LO}) if they match the energy separation of QD states.[1,23] For LO plus LA two-phonon processes sums over product terms $M_q^{\mathrm{LO}}M_k^{\mathrm{LA}}$ have to be calculated yielding relaxation rates of above 10^{11} s^{-1} according to Ref. 23, which is even larger than the observed relaxation rates.

To our knowledge multiphonon processes of higher order have not been calculated for QD's so far. But again it is important to realize that the emission times for single-phonon emission processes cannot just be added to give the emission time for the corresponding multiphonon process. Therefore, even a few of the ''slow'' LA phonons might participate in the measured fast relaxation of $\sim10^{10}$ s^{-1} at low temperature. Note in this context that the number of required LA phonons to cover an arbitrary energetic separation between excitation and detection energy by a LO-LA multiphonon process is reduced first by the possible interaction of QD carriers with the energetically different LO phonons of the GaAs bulk, the $In_xGa_{1-x}As$ wetting layer, the $In_xGa_{1-x}As$ QD's, and the respective interfaces (7 meV in Ref. 22) and second by broadening of these LO phonons due to strain and alloy inhomogeneities. Taking into account the Coulomb interaction between the electron and hole will further increase the number of possible combinations of LO and LA phonons to relax both the electron and hole energy: Phonon-assisted electron-hole scattering has been shown to allow a rapid transfer of the electron energy to the hole,[24] which means that the relaxation process of the electron-hole pair is limited only by the hole relaxation through its more dense energy spectrum.

B. Auger processes (high excitation density)

For time-averaged excitation densities I above 4 W/cm^2 the rise times under nonresonant excitation decrease with increasing excitation density and become independent of temperature at high excitation density (50 W/cm^2). Both properties are characteristic features of Auger processes.[25] The Auger scattering rates exceed the combined phonon capture and relaxation rates of $\sim10^{10}$ s^{-1} for $I>4$ W/cm^2 and

dominate the overall capture and relaxation rate at $I=50$ W/cm^2. Then the corrected barrier decay time τ_c describing the carrier capture into the QD's equals the nonresonant rise time τ_{r1} of the QD emission [Eq. (3)]. τ_{r1} reflects the carrier capture *and* relaxation. This can be explained by a single Auger process that is responsible for the carrier capture and carrier relaxation as illustrated in Fig. 8(b) for the electron. The electron (hole) is captured from the barrier directly into the QD ground state by transferring its energy to a second barrier electron (hole) next to the QD. However, we consider as well a sequence of two Auger processes displayed in Fig. 8(c): The electron is first captured into an excited QD state by Auger interaction with a second barrier electron and relaxes down to the QD ground state afterward, giving its energy to a third barrier electron or even more probably to another electron inside the QD. Note in this context that the onset of the decreasing PL rise times in Fig. 6 occurs at the same excitation density as the first observation of state filling. Equation (3) will be fulfilled for the Auger sequence if the Auger relaxation process is fast as compared to the Auger capture process. This has indeed been shown theoretically by Bockelmann and Egeler.[12] Since an Auger capture process into the QD ground state is expected to be slower than such a capture into excited QD states[12] the Auger sequence of Fig. 8(c) might be more efficient than the single Auger process of Fig. 8(b).

VI. CONCLUSION

Comparing PL rise times under resonant and nonresonant excitation with the decay times of the GaAs barrier allows us to separate and clearly identify the carrier capture and the carrier relaxation under low excitation density. We observe both fast capture and relaxation processes of the order of 10^{10} s^{-1} even in the one electron-hole pair per dot regime. The temperature dependence of the PL rise times reveals a different behavior at low and high excitation densities. We interpret our results in terms of multiphonon processes at low excitation densities. The temperature-dependent rise times indicate that acoustic phonons with energies that allow the maximum emission rates for the particular dot size to be realized are involved. The phonon wavelength is then comparable to the electron wavelength; typical acoustic-phonon energies of ~ 3 meV are small compared to the QD energy separations. At high excitation densities Auger processes can account for density-dependent and temperature-independent rise times that are no longer separable into capture and relaxation processes.

ACKNOWLEDGMENTS

We would like to thank T. Reinecke, A. Dite, V. Kulakovski, G. Bastard, and P. Lelong for valuable discussions and S. Kuhn for technical assistance.

[1] U. Bockelmann and G. Bastard, Phys. Rev. B **42**, 8947 (1990).
[2] P. A. Knipp and T. L. Reinecke, Phys. Rev. B **52**, 5923 (1995).
[3] H. Benisty, C. M. Sotomayor-Torres, and C. Weisbuch, Phys. Rev. B **44**, 10 945 (1991).
[4] K. Brunner, U. Bockelmann, G. Abstreiter, M. Walther, G. Böhm, G. Tränkle, and G. Weimann, Phys. Rev. Lett. **69**, 3216 (1992); U. Bockelmann, Phys. Rev. B **48**, 17 637 (1993).
[5] H. Lipsanen, M. Sopanen, and J. Ahopelto, Phys. Rev. B **51**, 13 868 (1995).
[6] J. Oshinowo, M. Nishioka, S. Ishida, and Y. Arakawa, Appl. Phys. Lett. **65**, 1421 (1994); M. Nishioka, J. Oshinowo, S. Ishida, and Y. Arakawa (unpublished).
[7] J.-Y. Marzin, J.-M. Gérard, A. Izrael, D. Barrier, and G. Bastard, Phys. Rev. Lett. **73**, 716 (1994).
[8] M. Grundmann, J. Christen, N. N. Ledentsov, J. Böhrer, D. Bimberg, S. S. Ruvimov, P. Werner, U. Richter, U. Gösele, J. Heydenreich, V. M. Ustinov, A. Yu. Egorov, A. E. Zhukov, P. S. Kop'ev, and Zh. I. Alferov, Phys. Rev. Lett. **74**, 4043 (1995).
[9] S. Fafard, R. Leon, D. Leonard, J. L. Merz, and P. M. Petroff, Phys. Rev. B **50**, 8086 (1994).
[10] G. Wang, S. Fafard, D. Leonard, J. E. Bowers, J. L. Merz, and P. M. Petroff, Appl. Phys. Lett. **64**, 2815 (1994).
[11] J.-M. Gérard, in *Confined Electrons and Photons: New Physics and Applications*, edited by E. Burstein and C. Weisbuch (Plenum, New York, 1995), pp. 357–381.
[12] U. Bockelmann and T. Egeler, Phys. Rev. B **46**, 15 574 (1992).
[13] H. Nakayama and Y. Arakawa, in *Quantum Electronics and Laser Science Conference, Baltimore, 1995*, OSA Technical Digest Series Vol. 5 (Optical Society of America, Washington, DC, 1995).
[14] G. Bastard and Ph. Lelong (unpublished).
[15] S. Fafard, R. Leon, D. Leonard, J. L. Merz, and P. M. Petroff, Phys. Rev. B **52**, 5752 (1995).
[16] S. Raymond, S. Fafard, S. Charbonneau, R. Leon, D. Leonard, P. M. Petroff, and J. L. Merz, Phys. Rev. B **52**, 17 238 (1995).
[17] At lower temperatures relaxation times are even longer in the 2D reference QW due to a localization of excitons requiring a relaxation via acoustic phonons from the 2D mobility edge. The exciton localization has been confirmed by measuring the exciton diffusion constant using an optical time-of-flight method.
[18] D. S. Citrin, Superlatt. Microstruct. **13**, 303 (1993).
[19] The nonresonant excitation energy used here is higher than the one used for the measurements of Fig. 3. However, the PL rise times are not considerably changed due to the fast carrier relaxation to the band gap in 3D GaAs. Excitation densities cannot be directly compared.
[20] P. Castrillo, D. Hessmann, M.-E. Pistol, S. Anand, N. Carlsson, and W. Seifert, Appl. Phys. Lett. **67**, 1905 (1995).
[21] H. Benisty, Phys. Rev. B **51**, 13 281 (1995).
[22] R. Heitz, M. Grundmann, N. N. Ledentsov, L. Eckey, M. Veit, D. Bimberg, V. M. Ustinov, A. Yu. Egorov, A. E. Zhukov, P. S. Kop'ev, and Zh. I. Alferov, Appl. Phys. Lett. **68**, 361 (1996).
[23] T. Inoshita and H. Sakaki, Phys. Rev. B **46**, 7260 (1992).
[24] Al. L. Efros, V. A. Kharchenko, and M. Rosen, Solid State Commun. **93**, 281 (1995).
[25] We exclude the influence of local heating of the lattice since PL rise times are unchanged when the laser beam is chopped.